Supplementary Materials and Methods

Terrestrial force production by the limbs of a semi-aquatic salamander provides insight into the evolution of terrestrial locomotor mechanics

Sandy M. Kawano and Richard W. Blob

Criteria for selecting trials for GRF measurements

Several criteria were used to determine whether a trial was valid for inclusion in our analyses. First, the entire right foot (fore or hind) needed to contact the force plate. Second, any portions of the data that had any body parts other than the limb of interest on the force plate were excluded from analysis. Third, only trials in which the complete limb cycle occurred during movement in a straight path across the force plate were considered (i.e., no turning or walking diagonally relative to the direction of the force plate). Trials were also excluded if the peak net GRF: 1) occurred at 0% or 100% of stance (since those patterns do not necessarily indicate a distinct maximum measurement), or 2) occurred at a time when more than the limb of interest was in contact with the force plate.

Experimental procedures

Data on three-dimensional GRF production of individual limbs walking over level ground were collected using procedures outlined in published studies by Blob and colleagues on fish, amphibians, reptiles, and mammals (Butcher & Blob, 2008; Sheffield & Blob, 2011; Sheffield et al., 2011; Butcher et al., 2011; Kawano & Blob, 2013). Briefly, data on the GRFs imposed on isolated appendages on the right side of the body were recorded (5000 Hz) using a custom-built, multi-axis force plate (K&N Scientific; Guilford, VT, USA) connected to bridge amplifiers. Two digitally synchronized, high-speed cameras (100 Hz; Phantom v.4.1, Vision Research Inc.; Wayne, NJ, USA) simultaneously filmed the dorsal and lateral views, with the dorsal view captured via a mirror positioned over the force plate at an angle of 45° to the trackway (Fig. 1). Data from the high-speed cameras and force plate were synchronized via a trigger that timed the onset of an LED light on the video with the onset of a 1.5 V pulse on the force traces.

GRF production by individual appendages was analyzed during stance, when the foot/fin is in contact with the ground and propulsion is generated. Since some of the force traces did not begin at a baseline of zero Newtons of force, data were padded by mirroring the data at the

beginning and end of the force trace to avoid edge effects during the filtering process. Padded force traces were then filtered using a low-pass, zero phase, second order Butterworth filter with the *signal* package in R (Signal developers, 2013). The order of the polynomial and the cut-off frequency were determined using the signal::buttord() function with the following filter specifications: 2500 Hz frequency, 0.0024 Hz passband frequency, 0.076 Hz stopband frequency, 2 dB passband ripple, and 40 dB stopband attenuation. These frequency values had been normalized to Nyquist frequency to avoid aliasing (Smith, 1997). Padding was removed prior to analysis. Data were then interpolated to 101 points to represent 1% increments, from 0% to 100%, during stance using a cubic spline with the signal::interp1('spline') function.

Filtered data were then used to calculate the magnitude and direction of the GRFs imposed upon the individual limbs during terrestrial locomotion. All force magnitudes were standardized to units of body weight (BW) to account for size differences across individuals and taxa. Magnitudes of the vertical, anteroposterior, and mediolateral components of the GRF were used to calculate the magnitude and orientation of the net GRF vector. Angular orientations were analyzed with respect to vertical (0°): positive values indicated a vector in the anterior or lateral directions and negative values indicated a vector in the posterior or medial directions.

Details on statistical analyses

Handling of data prior to statistical analyses

GRF magnitudes were converted to units of body mass and did not require further conversions to account for size differences among individuals. Angular measurements were also not standardized, as such steps could change the signs of angular values and drastically alter their biological interpretation (e.g., converting the orientation of the GRF from medial to lateral and, thereby, affecting moment arm calculations and estimations of bone loading regimes). Our other variables were continuous, did not include zeros, and did not differ in extreme orders of magnitude (standard errors were close to one or less), so these also were not standardized prior to analyses.

Other common rationales for standardizing data prior to statistical analyses also were not required for our purposes. For example, regression coefficients from the LMMs were not used to predict expected change in response variables for every change in unit of the explanatory variable (i.e., Appendage), so standardization was not necessary. Standardization may be required for models involving interactions (e.g., issues with collinearity can arise with interactions), but our LMMs included only a categorical variable as a fixed effect. Additionally,

since the factor levels within our categorical fixed effect are character strings, they do not contain numerical magnitudes that would weight one group as being more important than the others.

Testing assumptions of the linear mixed effects models (LMMs)

1) Linearity: Since the predictors are categorical, this assumption did not need to be tested.
2) Random sampling: individuals from each species were randomly selected for the study.
3) Normality of the residuals: Residuals were obtained from the LMM output from lme4::lmer() (Bates et al., 2015) and evaluated with Quantile-Quantile (Q-Q) plots using the qqplotr package (Almeida, Loy & Hofmann, 2017) in R.

Major violations of the test assumptions were not found for variables associated with the peak net GRF and yank. Points primarily fell within the confidence band of the Q-Q plot for each variable (Figures S1 – S3), suggesting that these variables reasonably met the assumption of normality. For the variables that showed some deviations from the confidence band, we re-ran the LMMs with the outliers removed (points that were 2x away from the interquartile range of the boxplot) and found that the “outliers” either had no effect on the fixed effects or made only ~4% or less of a difference (Table S1 – S2). At the most extreme, the “outliers” for positive yank in the mediolateral direction for the pelvic appendage decreased the fixed effect 13 – 18%. Thus, the full dataset was used for analysis in the main text since no major violations to the test assumptions were found.

Testing assumptions for peak net GRF data

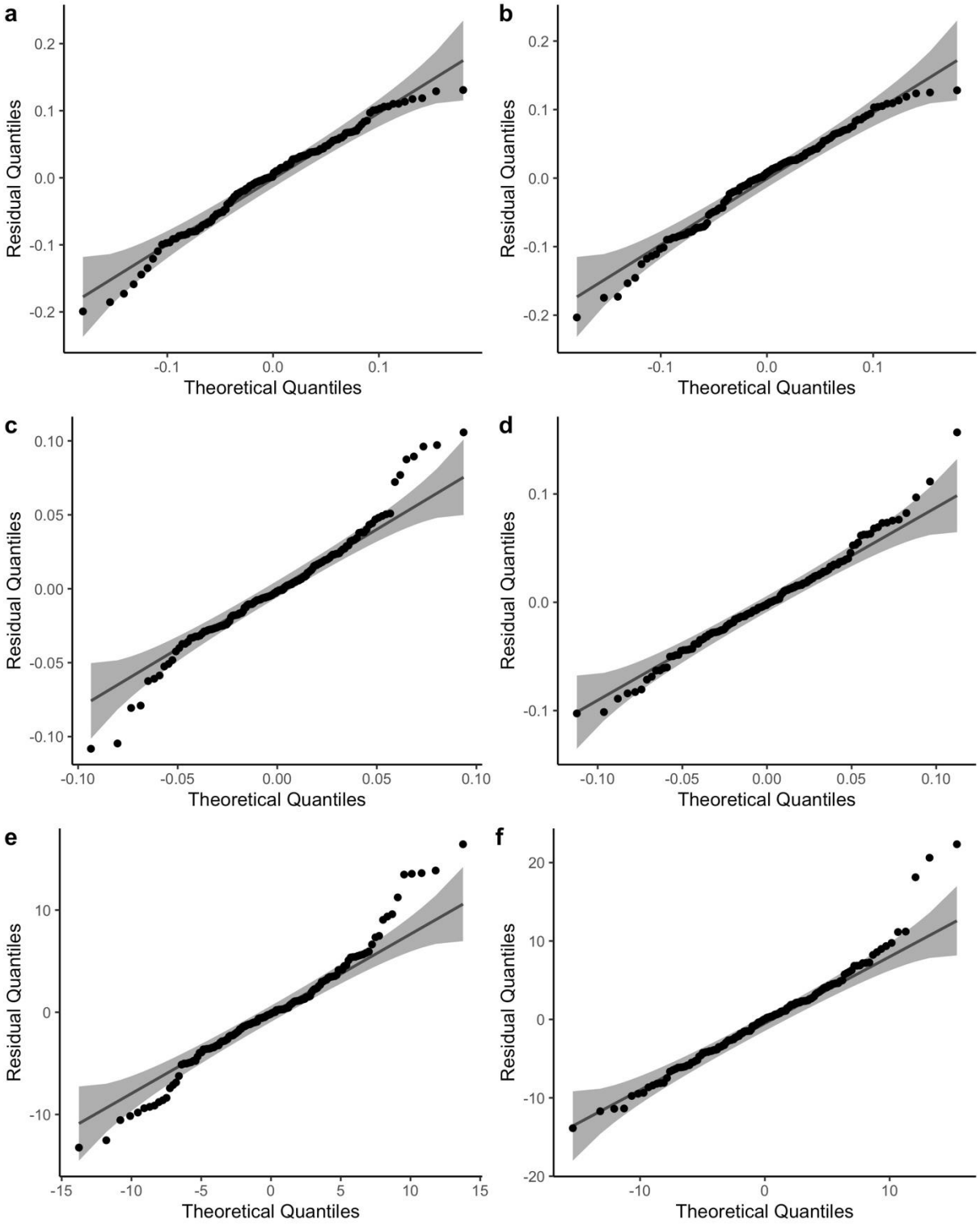

Fig. S1. Graphical assessments of normality in the pectoral LMM (n = 150 trials). The variables include a) net, b) vertical component, c) mediolateral component, d) anteroposterior component, e) mediolateral angle, and f) anteroposterior angle of the GRF. Most of the points fall within the confidence bands of the Q-Q plots for all variables, suggesting that the assumption of normality is reasonably met.

Table S1. Percent differences between the coefficients of the fixed effects produced from the full dataset versus a reduced dataset that has outliers removed for the peak net GRF.

	Full dataset		Dataset with outliers removed		
	FE ± s.e.	**CI**	**FE ± s.e.**	**CI**	**% diff**
Pec - ml					
A. tigrinum	-0.067 ± 0.012	-0.094, -0.041	-0.067 ± 0.0100	-0.089, -0.046	0
P. barbarus	-0.129 ± 0.012	-0.155, -0.102	-0.124 ± 0.0100	-0.149, -0.102	4
P. waltl	-0.087 ± 0.012	-0.114, -0.060	-0.089 ± 0.010	-0.111, -0.066	-2
Pec – ml angle					
A. tigrinum	-8.64 ± 1.36	-11.60, -5.66	-8.64 ± 1.22	-11.30, -5.97	0
P. barbarus	-17.04 ± 1.36	-20.0, -14.06	-16.76 ± 1.22	-19.40, -14.09	2
P. waltl	-13.62 ± 1.40	-16.7, -10.56	-13.91 ± 1.26	-16.70, -11.17	-2
Pec – ap angle					
A. tigrinum	-3.33 ± 1.60	-6.83, 0.16	-3.33 ± 1.71	-7.08, 0.412	0
P. barbarus	6.70 ± 1.64	3.21, 10.20	6.70 ± 1.71	2.96, 10.446	0
P. waltl	-12.38 ± 1.64	-15.95, -8.81	-12.94 ± 1.76	-16.75, -9.123	-4
Pel – ap angle					
A. tigrinum	16.7 ± 2.71	10.39, 22.90	16.1 ± 2.56	10.16, 22.00	4
P. waltl	14.9 ± 2.72	8.59, 21.10	14.9 ± 2.56	8.96, 20.80	0

Testing assumptions for yank data

Maximum yank

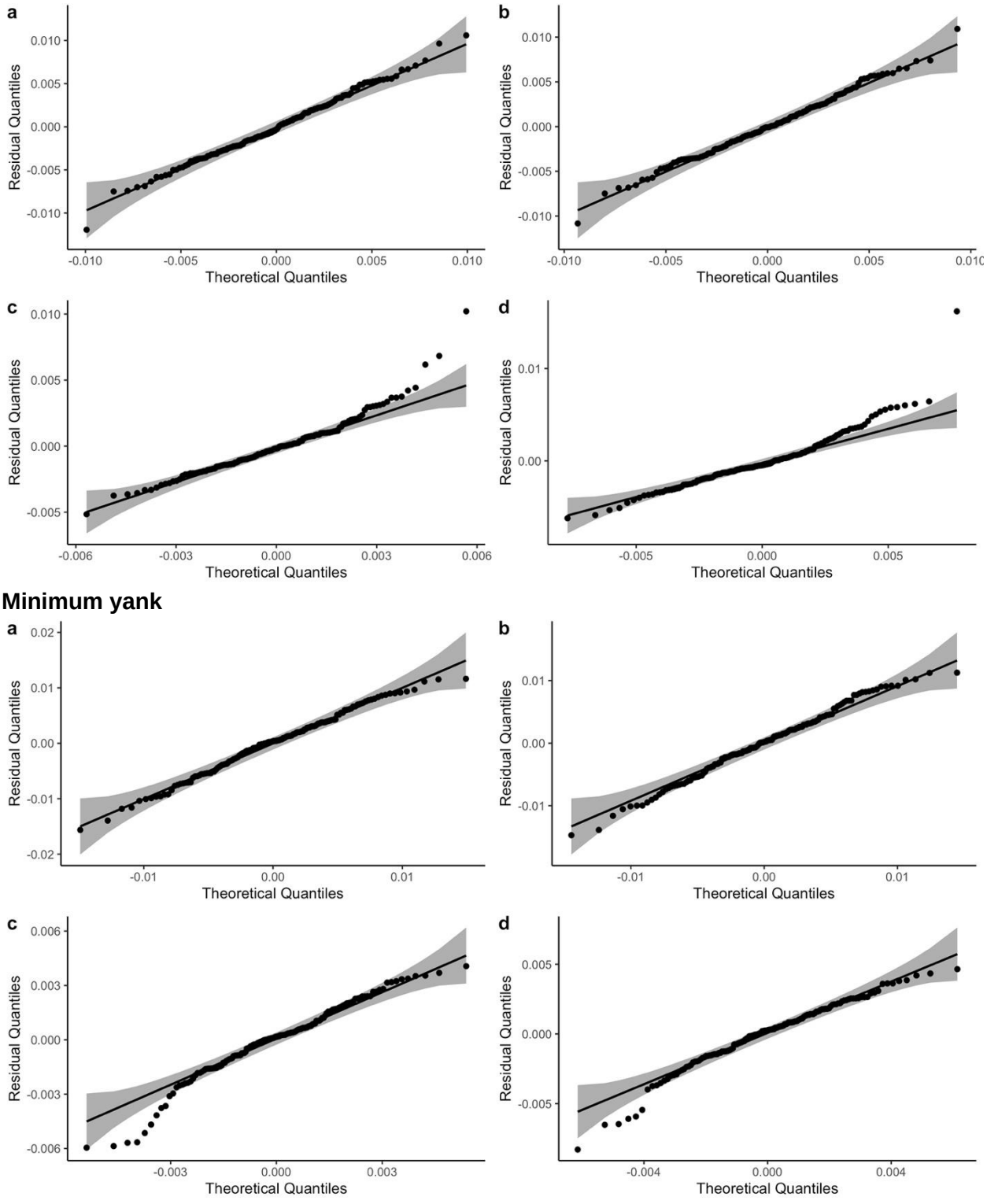

Minimum yank

Fig. S2. QQ plots of maximum and minimum yank values for the a) net, b) vertical component, c) mediolateral component, and d) anteroposterior component of the GRF produced by the pectoral appendages.

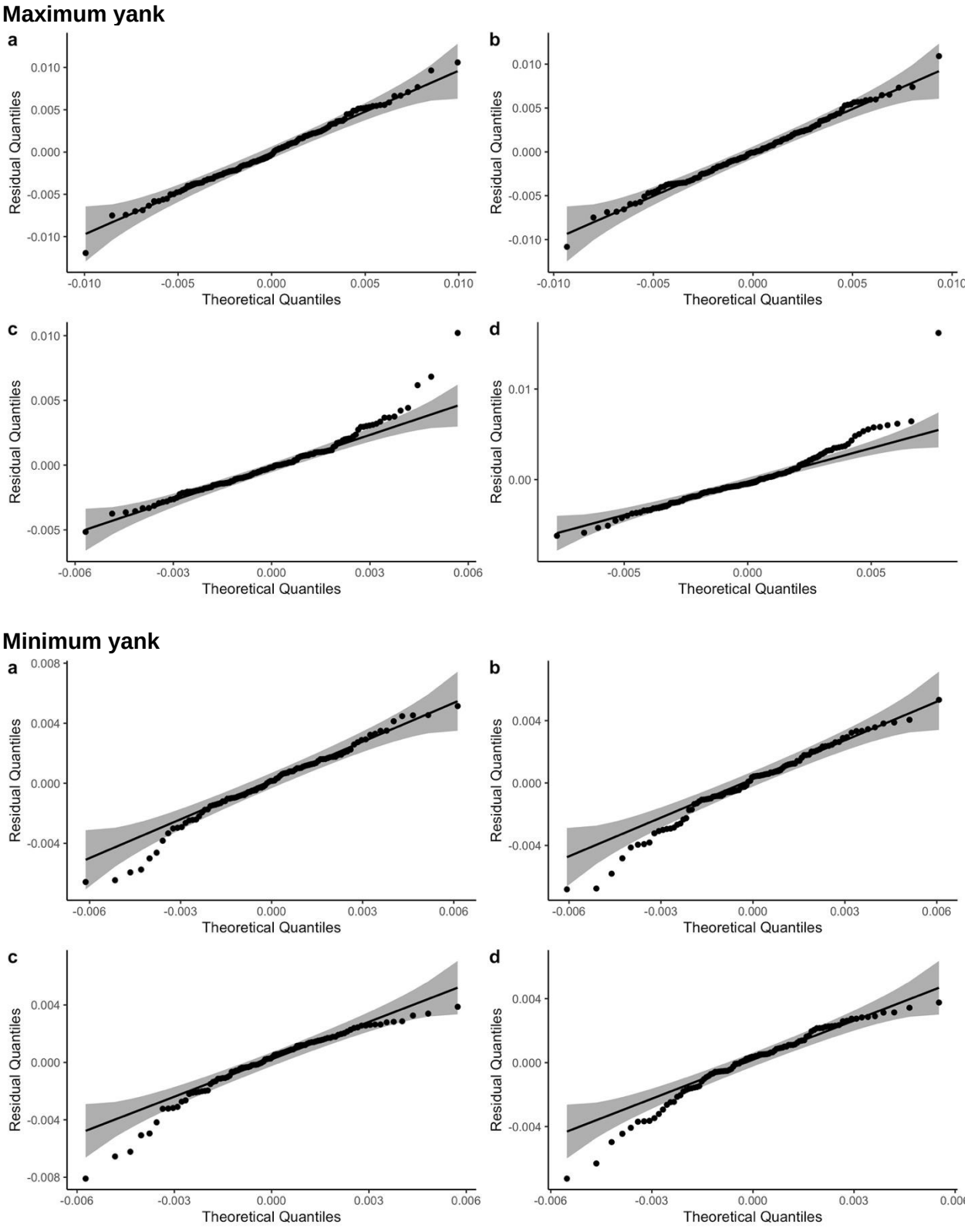

Fig. S3. QQ plots of the maximum and minimum yank values for the a) net, b) vertical component, c) mediolateral component, and d) anteroposterior component of the GRF produced by the pelvic appendages.

Table S2. Percent differences between the coefficients of the fixed effects produced from the full dataset versus a reduced dataset that has outliers removed for the yank data

	Full dataset		Dataset with outliers removed		
	FE ± s.e.	**CI**	**FE ± s.e.**	**CI**	**% diff**
Pec – max - ml					
A. tigrinum	0.0036 ± 0.0007	0.0020, 0.0052	0.0036 ± 0.0006	0.0023, 0.0049	0
P. barbarus	0.0044 ± 0.0007	0.0028, 0.0060	0.0042 ± 0.0006	0.0029, 0.0055	5
P. waltl	0.0060 ± 0.0007	0.0044, 0.0076	0.0058 ± 0.0006	0.0045, 0.0072	3
Pec – max - ap					
A. tigrinum	0.0059 ± 0.0007	0.0044, 0.0075	0.0059 ± 0.0006	0.0046, 0.0073	0
P. barbarus	0.0037 ± 0.0007	0.0022, 0.0053	0.0037 ± 0.0006	0.0024, 0.0051	0
P. waltl	0.0082 ± 0.0007	0.0066, 0.0098	0.0079 ± 0.0006	0.0065, 0.0092	4
Pec – min - ml					
A. tigrinum	-0.0042 ± 0.0006	-0.0056, -0.0028	-0.0041 ± 0.0005	-0.0052, -0.0029	2
P. barbarus	-0.0049 ± 0.0006	-0.0063, -0.0035	-0.0046 ± 0.0005	-0.0058, -0.0035	7
P. waltl	-0.0063 ± 0.0007	-0.0078, -0.0049	-0.0063 ± 0.0005	-0.0075, -0.0051	0
Pec – min – ap					
A. tigrinum	-0.0066 ± 0.0006	-0.0080, -0.0052	-0.0063 ± 0.0006	-0.0075, -0.0051	5
P. barbarus	-0.0039 ± 0.0006	-0.0052, -0.0025	-0.0039 ± 0.0006	-0.0051, -0.0027	0
P. waltl	-0.0045 ± 0.0006	-0.0059, -0.0031	-0.0045 ± 0.0006	-0.0058, -0.0033	0
Pel – max - v					
A. tigrinum	0.0096 ± 0.0013	0.0066, 0.0127	0.0096 ± 0.0013	0.0066, 0.0127	0
P. waltl	0.0052 ± 0.0013	0.0021, 0.0082	0.0047 ± 0.0013	0.0017, 0.0078	11
Pel – max - ap					
A. tigrinum	0.0087 ± 0.0009	0.0067, 0.0107	0.0077 ± 0.0006	0.0064, 0.0090	13
P. waltl	0.0060 ± 0.0009	0.0040, 0.0080	0.0051 ± 0.0006	0.0038, 0.0065	18
Pel – max - net					
A. tigrinum	0.0105 ± 0.0013	0.0074, 0.0135	0.0105 ± 0.0014	0.0074, 0.0136	0
P. waltl	0.0058 ± 0.0013	0.0027, 0.0088	0.0055 ± 0.0014	0.0023, 0.0086	7
Pel – min – ml					
A. tigrinum	-0.0042 ± 0.0004	-0.0052, -0.0033	-0.0041 ± 0.0004	-0.0050, -0.0032	2
P. waltl	-0.0044 ± 0.0004	-0.0053, -0.0034	-0.0042 ± 0.0004	-0.0051, -0.0033	5
Pel – min – ap					
A. tigrinum	-0.0070 ± 0.0006	-0.0083, -0.0057	-0.0068 ± 0.0005	-0.0078, -0.0057	3
P. waltl	-0.0061 ± 0.0006	-0.0074, -0.0048	-0.0061 ± 0.0005	-0.0072, -0.0050	0

Comparison of stance durations

When we ran a species x stance duration interaction term as a fixed effect in our LMMs, stance duration was a good predictor in only the anteroposterior component and angle of the GRF for the pectoral appendages. The interaction between *P. barbarus* and stance duration was important for the mediolateral component, anteroposterior component, and anteroposterior angle of the GRF, so we report results for these comparisons as well. Comparisons of the point estimates for the species between our reduced and full models indicated that including stance duration in our LMMs had minimal to no effect for almost all variables (Table S3). Point estimates between the reduced and full models differed by less than 2 degrees for the mediolateral and anteroposterior angles of the GRF but had overlapping confidence intervals, suggesting these differences were negligible (Table S3). The mediolateral components of the GRF were equivalent between the reduced and full models for the salamanders but was 0.019 BW lower in the full model for *P. barbarus*, which only strengthened one of the main findings in our study. The anteroposterior component of the GRF had the most pronounced differences between the reduced and full models but did not affect the main patterns found in our results. Salamander forelimbs became slightly (10 – 20 %) more deceleratory and mudskipper pectoral fins became moderately less acceleratory (25%).

Table S3. Comparison of locomotor variables between the pectoral appendages of mudskippers and salamanders at the peak net GRF with and without stance duration as a fixed effect

	Periophthalmus barbarus n = 50		*Pleurodeles waltl* n = 50		*Ambystoma tigrinum* n = 50	
	FE ± s.e.	CI	FE ± s.e.	CI	FE ± s.e.	CI
Net GRF (BW)						
Excluding stance duration	0.443 ± 0.014	0.412, 0.473	0.404 ± 0.015	0.372, 0.436	0.458 ± 0.014	0.427, 0.488
Including stance duration	0.448 ± 0.018	0.410, 0.486	0.407 ± 0.016	0.372, 0.442	0.462 ± 0.015	0.429, 0.495
Vertical GRF (BW)						
Excluding stance duration	0.417 ± 0.012	0.392, 0.442	0.381 ± 0.012	0.355, 0.407	0.447 ± 0.012	0.422, 0.473
Including stance duration	0.411 ± 0.013	0.383, 0.439	0.384 ± 0.013	0.356, 0.412	0.450 ± 0.012	0.423, 0.476
Mediolateral GRF (BW)						
Excluding stance duration	-0.129 ± 0.012	-0.115, -0.102	-0.087 ± 0.013	-0.114, -0.060	-0.067 ± 0.012	-0.094, -0.041
Including stance duration	-0.148 ± 0.013	-0.176, -0.120	-0.086 ± 0.012	-0.112, -0.059	-0.067 ± 0.012	-0.093, -0.041
Anteroposterior GRF (BW)						
Excluding stance duration	0.048 ± 0.013	0.020, 0.076	-0.086 ± 0.013	-0.115, -0.057	-0.029 ± 0.013	-0.058, -0.001
Including stance duration	0.036 ± 0.014	0.006, 0.066	-0.095 ± 0.013	-0.124, -0.066	-0.035 ± 0.013	-0.063, -0.007
Mediolateral angle (°)						
Excluding stance duration	-17.04 ± 1.36	-20.00, -14.06	-13.62 ± 0.140	-16.70, -10.56	-8.64 ± 1.36	-11.60, -5.66
Including stance duration	-17.91 ± 1.47	-21.10, -14.74	-13.13 ± 1.47	-16.30, -9.93	-8.29 ± 1.43	-11.40, -5.18
Anteroposterior angle (°)						
Excluding stance duration	6.70 ± 1.60	3.21, 10.20	-12.38 ± 1.64	-15.95, -8.81	-3.33 ± 1.60	-6.83, 0.16
Including stance duration	5.09 ± 1.70	1.53, 8.65	-13.64 ± 1.56	-17.00, -10.28	-4.23 ± 1.49	-7.48, -0.99

Statistical analyses were based on the model: lmer(y ~ Species + (1|Individual), REML=True) when excluding stance duration or lmer(y ~ Species*stance_s + (1|Individual), REML=True) when including stance duration. Fixed effect (FE) values, standard errors, and confidence interval (CI) were estimated from the linear mixed effects model using the emmeans R package. The interaction between species and stance duration was evaluated at the average stance duration (0.487 secs). $R^2_{LMM(m)}$ represents the variance explained by the fixed effects whereas $R^2_{LMM(c)}$ represents the variance explained by the combination of fixed and random effects, and were calculated using the performance::r2_nakagawa() function in R.

REFERENCES

Almeida A, Loy A, Hofmann H. 2017. *qqplotr: Quantile-Quantile Plot Extensions for "ggplot2". R package version 0.0.3 initially funded by Google Summer of Code 2017. https://github.com/aloy/qqplotr.*

Ashley-Ross MA. 1994. Hindlimb kinematics during terrestrial locomotion in the salamander (*Dicamptodon tenebrosus*). *Journal of Experimental Biology* 193:285–305.

Ashley-Ross MA, Barker JU. 2002. The effect of fiber-type heterogeneity on optimized work and power output of hindlimb muscles of the salamander Ambystoma tigrinum. *Journal of Comparative Physiology A* 188:611–620. DOI: 10.1007/s00359-002-0336-4.

Ashley-Ross MA, Lundin R, Johnson KL. 2009. Kinematics of level terrestrial and underwater walking in the California newt, *Taricha torosa*. *Journal of Experimental Zoology* 311A:240–257. DOI: 10.1002/jez.522.

Bates D, Maechler M, Bolker B, Walker S. 2015. Fitting linear mixed-effects models using lme4. *Journal of Statistical Software* 67:1–48. DOI: doi:10.18637/jss.v067.i01.

Bennett AF, Garland T, Else PL. 1989. Individual correlation of morphology, muscle mechanics, and locomotion in a salamander. *The American journal of physiology* 256:1200–1208.

Butcher MT, Blob RW. 2008. Mechanics of limb bone loading during terrestrial locomotion in river cooter turtles (*Pseudemys concinna*). *The Journal of experimental biology* 211:1187–1202. DOI: 10.1242/jeb.012989.

Butcher MT, White BJ, Hudzik NB, Gosnell WC, Parrish JHA, Blob RW. 2011. In vivo strains in the femur of the Virginia opossum (*Didelphis virginiana*) during terrestrial locomotion: testing hypotheses of evolutionary shifts in mammalian bone loading and design. *The Journal of experimental biology* 214:2631–2640. DOI: 10.1242/jeb.049544.

Canoville A, Laurin M. 2009. Microanatomical diversity of the humerus and lifestyle in lissamphibians. *Acta Zoologica* 90:110–122. DOI: 10.1111/j.1463-6395.2008.00328.x.

Deban SM, Schilling N. 2009. Activity of trunk muscles during aquatic and terrestrial locomotion in *Ambystoma maculatum*. *The Journal of experimental biology* 212:2949–59. DOI: 10.1242/jeb.032961.

Delvolvé I, Bem T, Cabelguen JM. 1997. Epaxial and limb muscle activity during swimming and terrestrial stepping in the adult newt, *Pleurodeles waltl*. *Journal of neurophysiology* 78:638–50.

Karakasiliotis K, Schilling N, Cabelguen J-M, Ijspeert AJ. 2012. Where are we in understanding salamander locomotion: biological and robotic perspectives on kinematics. *Biological Cybernetics* 107:529–544. DOI: 10.1007/s00422-012-0540-4.

Kawano SM, Blob RW. 2013. Propulsive forces of mudskipper fins and salamander limbs during terrestrial locomotion: implications for the invasion of land. *Integrative and comparative biology* 53:283–294. DOI: 10.1093/icb/ict051.

Laurin M, Girondot M, Loth M-M. 2004. The evolution of long bone microstructure and lifestyle in lissamphibians. *Paleobiology* 30:589–613.

Obst FJ, Richter K, Jacon U. 1988. *The completely illustrated atlas of reptiles and amphibian for the terrarium*. Neptune City, NJ: T.F.H. publications.

Petranka JW. 1998. *Salamanders of the United States and Canada*. Washington, D.C.: Smithsonian Institution Press.

Pierce SE, Hutchinson JR, Clack JA. 2013. Historical perspectives on the evolution of tetrapodomorph movement. *Integrative and Comparative Biology* 53:209–23. DOI: 10.1093/icb/ict022.

Sheffield KM, Blob RW. 2011. Loading mechanics of the femur in tiger salamanders (*Ambystoma tigrinum*) during terrestrial locomotion. *Journal of Experimental Biology* 214:2603–2615. DOI: 10.1242/jeb.048736.

Sheffield KM, Butcher MT, Shugart SK, Gander JC, Blob RW. 2011. Locomotor loading mechanics in the hindlimbs of tegu lizards (*Tupinambis merianae*): comparative and evolutionary implications. *Journal of Experimental Biology* 214:2616–2630. DOI: 10.1242/jeb.048801.

Signal developers. 2013.signal: Signal processing. *Available at http://r-forge.r-project.org/projects/signal/.*

Smith S. 1997. *The scientist and engineer's guide to digital signal processing*. San Diego, CA: California Technical Publishing.

Stokely PS, Holle PA. 1954. Appendicular skeleton of the Ambystomidae. *Herpetologica* 10:57–61.

Wake DB. 2009. What salamanders have taught us about evolution. *Annual Review of Ecology, Evolution, and Systematics* 40:333–352. DOI: 10.1146/annurev.ecolsys.39.110707.173552.